

Microscale Laser Shock Processing (LSP) of Metal Thin Films

Wenwu Zhang* and Y. Lawrence Yao

Department of Mechanical Engineering

Columbia University, New York, NY 10027

* Currently with General Electric Global Research Center

Abstract

Microscale Laser Shock Processing (LSP) is a technique that may be potentially used to manipulate the residual stress distributions in metal film structures and thus improve the reliability performances of micro-devices. In this study, microscale LSP of copper thin films on single crystal silicon substrates is investigated. Curvature measurements verify that substantial average compressive residual stress can be induced in copper thin films using microscale LSP. High spatial resolution is required to measure the stress/strain field in microscale LSP. For the first time, X-ray microdiffraction technique based on diffraction intensity contrast method is used to measure the relative variation of the stress/strain field in the shock treated copper thin films. The experimental results are further understood through 3D FEM analysis.

1 Introduction

Failure and reliability problems in MEMS have attracted increasing concerns recently. While the dominant material in MEMS is silicon, metal and metallic thin film structures are often indispensable, and metal is a better choice for some applications. Wearing of rubbing surfaces is the major cause of failure for silicon-based micro-engines, while tungsten-coated polysilicon micro-engines show much higher wear resistance than pure polysilicon structures (Walraven et al., 2000). Aluminum thin film microwave switch was demonstrated to have very low current loss due to its small dimension and its metal structure (Chang & Chang, 2000). These metallic thin film structures are typically made by patterning the thin film first and then sacrificing part of the supporting substrate. Some of these metal microstructures, such as micro-electromechanical actuators, metal gears, and metal switches, experience cyclic loads in service. Wear resistance and fatigue performance of these metal structures should be improved to increase the reliability of the system.

Microscale Laser Shock processing (LSP) can efficiently induce favorable residual stress distributions in bulk metal targets with micron-level spatial resolution (Zhang and Yao, 2002). It may potentially be used to improve the wear resistance and fatigue performance of metal film structures. In LSP, a short and intense ($>1 \text{ GW/cm}^2$) laser pulse is irradiated through the confining medium (such as water) onto a metallic surface, which is applied with a sacrificial coating (organic paint, tape, or thin metallic foil), and the coating is instantaneously vaporized and evolves into a rapidly expanding plasma plume. This plasma induces shock waves during expansion from the irradiated surface, and a rapidly rising high-pressure shock wave propagates to the target. When the peak shock pressure is over the Hugoniot Elastic Limit of the metal for a

suitable time, the metal yields and is plastically deformed, resulting in compressive surface residual stress.

To apply microscale LSP to metallic components in microsystems, it is necessary to understand how the thin film material on silicon substrate responds to LSP. The application of microscale LSP to metal films with a thickness less than 10 microns has not been studied in the literature. The microscale also poses challenges in terms of material characterization. Recent advances in x-ray microdiffraction offer promise of measuring residual stress with micron spatial resolution and need to be investigated. In this study, simulation and experimental investigation of microscale LSP of copper thin films on silicon substrates are presented.

2 Average Stress Measurement Using the Wafer Curvature Method

Curvature measurements are carried out to answer the question of whether microscale LSP can induce compressive residual stress in metal thin films. The samples are $1\mu\text{m}$ and $3\mu\text{m}$ copper films on 1" round single crystal silicon wafers with (001) orientation and 0.254mm thickness. The $1\mu\text{m}$ samples are prepared by PVD at a chamber pressure of 2mTorr. The $3\mu\text{m}$ samples are prepared by electrochemical plating. A Q-switched Nd:YAG laser with pulse duration of 50ns and wavelength of 355nm is used in the shock experiments. During laser shock processing, the sample is covered with an aluminum foil of $16\mu\text{m}$ thickness, with a very thin layer of vacuum grease in between. Thus, thermal effects are isolated and only shock effects are experienced by the sample.

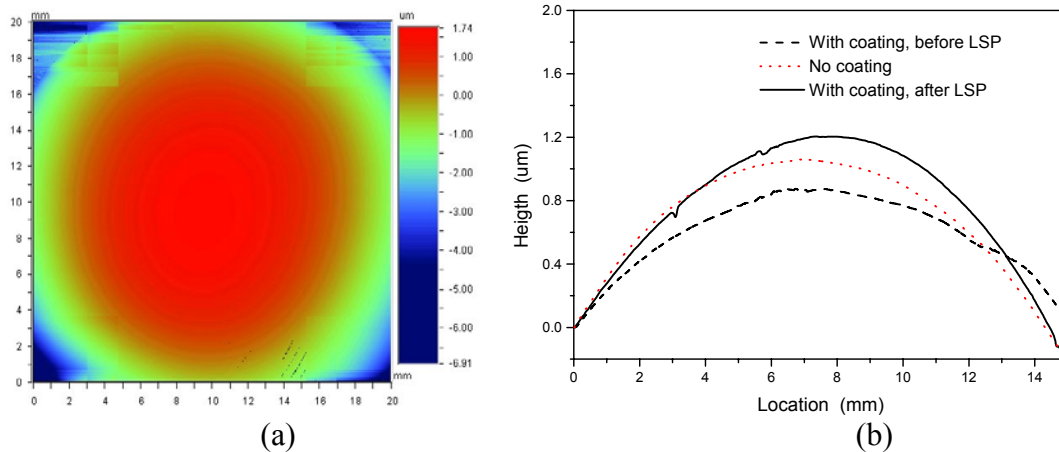


Fig. 1 Curvature measurement of the $1\mu\text{m}$ sample (a) 2D contours of the wafer surface, after LSP; and (b) Surface profile variations.

Six lines (10mm in length and 2mm in spacing) of shocks are applied across the central part of the wafer, and three laser pulses (pulse energy = $244\mu\text{J}$) are applied at each location separated by $25\mu\text{m}$. The curvatures of the wafers before coating, and after coating with and without laser shock processing are measured using an optical profiler (Wyko 3300). The average residual stress in the thin films on the silicon substrates can be computed according to (Segmüller et al., 1980):

$$\sigma_f = \frac{M_s t_s^2}{6 t_f} (1/R - 1/R_0) \quad (1)$$

where t_s and t_f are the thickness of the substrate and the film, respectively, R and R_0 the current and original wafer radius (seen from the film side), respectively, and M_s the biaxial modulus of the substrate. For the (001) single crystal silicon wafer, $M_s = 180.5\text{GPa}$ (Segmüller et al., 1980). Fig. 1(a) shows the 2D contours of the $1\mu\text{m}$ sample after LSP measured with an optical profiler. Curvature of the wafer can be measured from the profiles, as shown in Fig. 1(b). Copper has a larger expansion coefficient than silicon. After coating and cooling down, the copper film contracts more than the silicon substrate. Thus, the copper film experiences tensile stress. The substrate close to the film experiences compressive stress due to force balance. As a result, the initially convex curvature of the wafer becomes less convex when the film stress is tensile. On the other hand, when the film stress is compressive, the wafer surface will become more convex. This explains the profile changes in Fig. 1(b). The profile becomes less convex after coating due to tensile stress, and becomes more convex after LSP due to LSP induced compressive residual stress in the film.

The film stress after coating increases with the increase in film thickness. Tensile stress tends to make the wafer more concave. Using Eq. (1), the residual stress variations in the thin films are computed. Both $1\mu\text{m}$ and $3\mu\text{m}$ samples show tensile residual stresses after coating, and both change to compressive after laser shock processing. Considering that only six lines of shock loads are applied on the film surface, and that an average compressive residual stress of more than 35MPa is generated after laser shock processing, it is concluded that microscale LSP can induce substantial compressive residual stresses in metal thin films on silicon substrates. Curvature measurement can only estimate the average stress in the thin film. To study the local distribution of the stress/strain field, however, simulation and high spatial resolution experimental work should be carried out.

3 Stress/Strain Analysis

3.1 Special Considerations in the Simulation of Layered Thin Film Structures

Microscale LSP of bulk copper and nickel foils had been studied (Zhang and Yao, 2001), and the simulation results based on self-developed LSP model were validated by the measurement of shock induced dent geometries. In this study, 3D stress/strain analysis of copper thin films on silicon substrates is carried out under similar loading conditions as the samples used in the experiments to further the understanding of the experimental results. The silicon substrate is treated as elastic and isotropic. The computed shock pressure is used as boundary conditions in the stress/strain analysis.

Stress/strain analysis of a layered structure should consider the stress coupling, contact condition and relative motion of the interfaces. Cohesion and debonding are important when the interface is under tension and shear. In this research, the samples were prepared through sputtering PVD and electrochemical plating. The samples were carefully monitored to make sure that the films were well adhered to the substrates. In the experiments, all shock loads were

applied to the central part of the film from the copper film side, and the normal stress at the interface is compressive most of the time. For this reason, no separation of interface occurred in any of the experiments. The high quality binding in the central region of the film makes the tangential sliding very small if sliding does occur. Thus, in these preliminary simulations, tangential sliding is neglected, and the interfaces are assumed to be perfectly bonded. Interfaces in perfect contact obviate the need to consider additionally the dynamic process in LSP.

The interface algorithm is implemented in the commercial FEM package Abaqus. Only a quarter of the shocked sample needs to be computed due to symmetry, and the selected computation domain is 200 microns in 11-direction and 300 microns in 22-direction (Fig. 2(a)). The silicon substrate is 20 microns in thickness, while the copper thin film has a thickness of 1, 1.5 or 3 microns. A line of shocks with 25 micron spacing is applied on the top surface along the centerline (22-direction), and the shocked region is 225 microns in length, 75 microns away from the sample edge. The bottom surface of the silicon substrate is fixed in position. The internal side surfaces are symmetric about the 11 and 22-axes, respectively, and the two external edges are traction free.

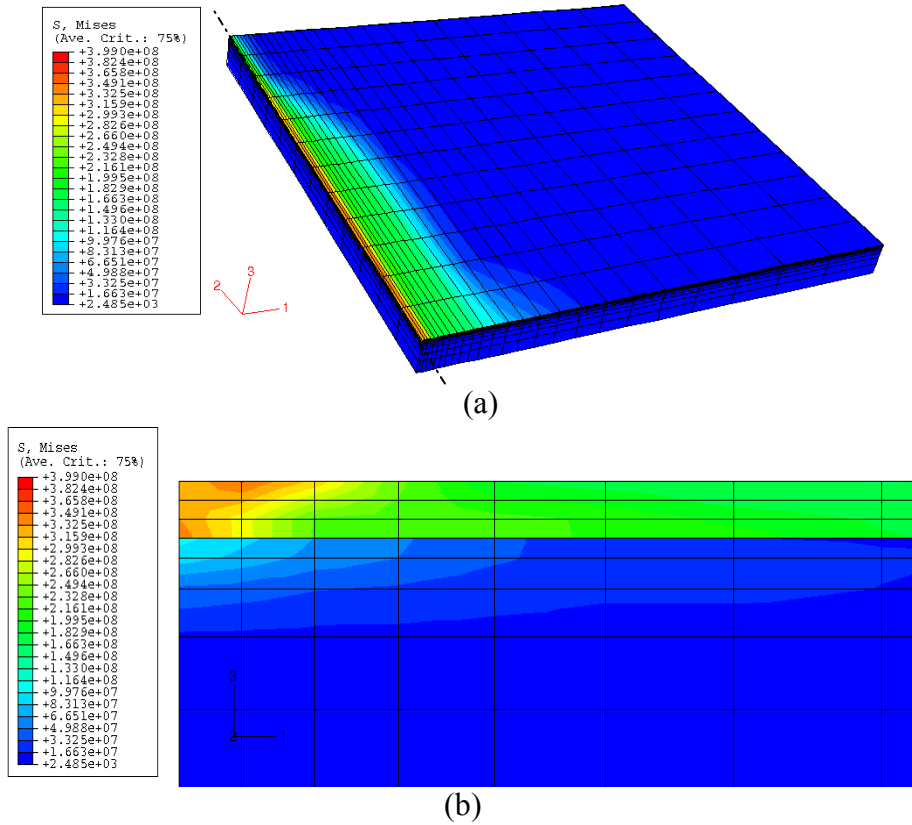


Fig. 2 Distribution of the von Mises stress, 1 μ m sample at 244 μ J (a) 3D overview; and (b) detailed view of the interface along the cross section;. Only the layers close to the interface are shown. The centerline is shown in Fig. 10(a). Cross sections are perpendicular to the centerline.

3.2 Simulation Results and Discussion

Fig. 2(a) shows the 3D von Mises stress distribution after laser shock processing of the 1 μ m sample at 244 μ J. The von Mises stress indicates the region of stress concentration. A line

of shocks applied along the centerline of the sample influences a region about 75microns on either side of the centerline. The stress/strain fields are approximately uniform along lines parallel to the 22-direction, except in the shocked-free region close to the edge. Thus, a cross section profile in the following analysis can reflect the stress/strain distributions in a large area.

Stress/strain coupling at the interface is of special interest in order to understand the experimental results in X-ray diffraction. Fig. 2(b) shows in detail the stress coupling at the copper-silicon interface along the cross section. The top three layers are copper. It is seen that the von Mises stress in copper changes from high to low away from the centerline. Stress is nearly uniform in the whole thickness of the film, except in the region close to the center ($<10\text{microns}$). Stress distribution in silicon spans a narrower range than in copper along the cross section, and only a very thin layer (about 1 micron) of silicon near the interface is affected.

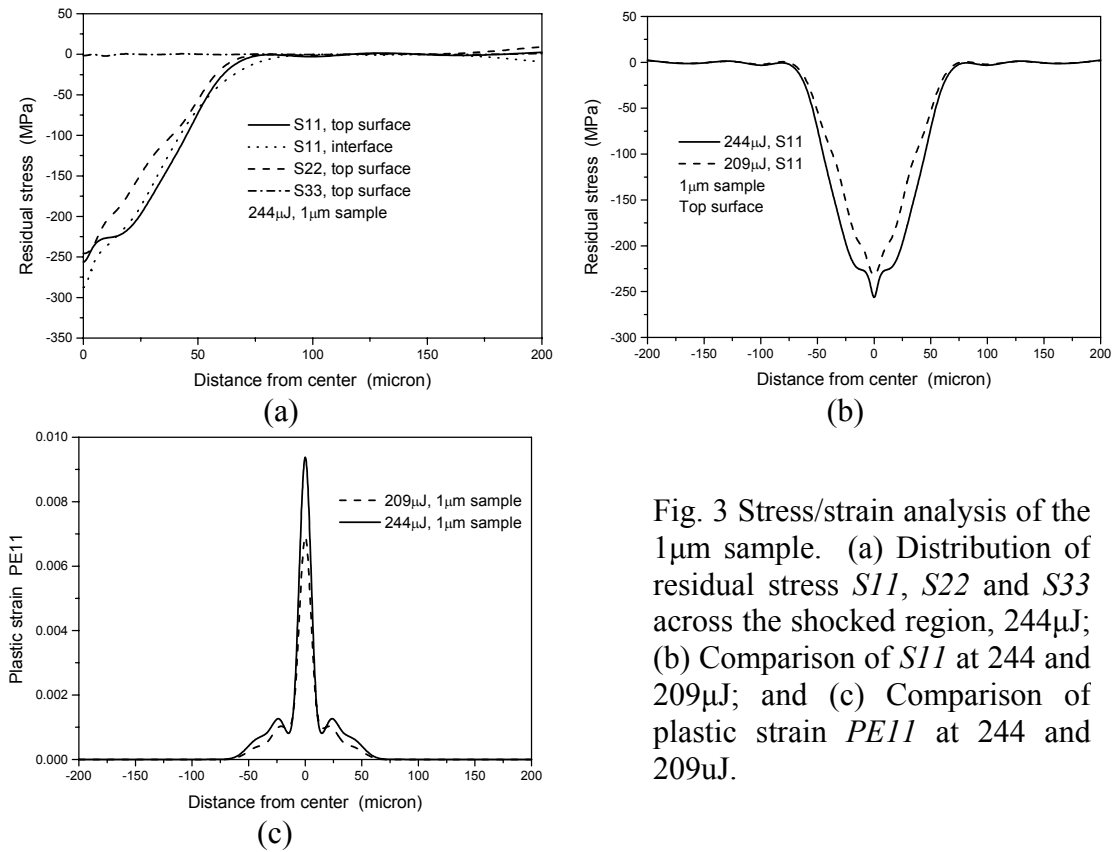


Fig. 3 Stress/strain analysis of the $1\mu\text{m}$ sample. (a) Distribution of residual stress $S11$, $S22$ and $S33$ across the shocked region, $244\mu\text{J}$; (b) Comparison of $S11$ at 244 and $209\mu\text{J}$; and (c) Comparison of plastic strain $PE11$ at 244 and $209\mu\text{J}$.

Simulation results in Fig. 3(a) show that on the top surface along the cross section of the sample, the values of the in-plane stress $S11$ and $S22$ are close, and in-depth stress $S33$ is nearly zero everywhere. Thus, the stress distribution in the film is close to equi-biaxial. The value of $S11$ at the interface is compared with the value on the top surface. It is seen that except in a narrow range near the centerline ($<10\text{microns}$), $S11$ is nearly uniform within the whole depth of the film. The distributions of top-surface residual stress $S11$ for the $1\mu\text{m}$ sample at $244\mu\text{J}$ ($4.31\text{GW}/\text{cm}^2$) and $209\mu\text{J}$ ($3.67\text{GW}/\text{cm}^2$) are compared in Fig. 3(b). Within 50microns from the center, the in-plane stress is compressive and larger than 100MPa . Although the increase of compressive residual stress (-225 to -250MPa) is not substantial when the energy is increased from $209\mu\text{J}$ to $244\mu\text{J}$, plastic strain $PE11$ has a substantial increase as seen in Fig. 3(c). Plastic

strain PE_{11} and PE_{22} in copper are nearly equal. Thus, although the increased energy does not increase the residual stress substantially, it is dissipated through plastic deformation.

4 Characterization of the Stress/Strain Fields Using X-ray Microdiffraction

4.1 Principles of Measurement

The spatial resolution of normal X-ray diffraction is typically larger than 0.5mm, which has been used to measure the average stress/strain but is too large to measure the stress/strain distributions in microscale laser shock processing (Zhang and Yao, 2002). Recent developments in X-ray microdiffraction provide the possibility of measuring the stress/strain fields with micron-level spatial resolution. The high brightness X-ray beams from synchrotron radiation sources are narrowed down and then focused to micron or submicron spot sizes using X-ray optics such as Fresnel Zone Plates (FZP) or tapered glass capillaries, and either white beam or monochromatic X-rays are used. Due to the divergence and uneven intensity distribution of the incident X-rays, and due to the insufficient number of grains sampled at each test point, the uncertainty of the Bragg angle may be too large to determine the absolute values of the lattice spacing (Noyan et al. 2000). On the other hand, relative stress/strain variations can be reliably characterized with micron-level spatial resolution by recording the diffraction intensity contrast of the underlying single crystal silicon substrate (Noyan et al., 1998; Wang et al., 2000). The diffraction intensity contrast method will be used in this study.

In the diffraction intensity contrast method, the X-ray microbeam penetrates the top thin film layer (usually polycrystalline) and the diffraction intensity of the single crystal substrate is recorded. The stress/strain in the thin film is coupled to and deforms the substrate. Laser shock peening induces local stress/strain in the single crystal substrate. The strained region induces mosaic structures, while the strain-free region is close to perfect crystal. Due to the increased bandwidth of strong diffraction and the reduced extinction processes, the integrated X-ray diffraction intensity increases in the locally strained region compared with the strain-free region. A single crystal substrate is necessary in this method, and the film layer should be thin enough to get strong diffraction signals.

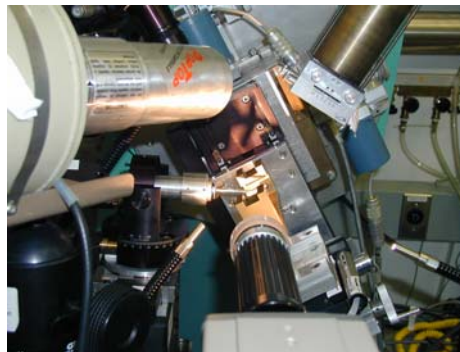


Fig. 4 Experimental setup of the X-ray Microdiffraction Experiment (Courtesy of Steffen Kaldor)

Fig. 4 shows the setup of the X-ray microdiffraction experiment. Experiments were conducted at IBM's X20A beamline of the National Synchrotron Light Source at Brookhaven National Laboratory. First, fluorescence tests were carried out using 9.1KeV beam energy to monitor the surface integrity of the sample. Then monochromatic X-rays at 8.5 KeV ($\lambda=1.459$ Å) were used in the diffraction tests. The incident X-ray beams were focused using a tapered glass capillary to form a 10micron by 10micron spot on the sample surface. Si (004) diffraction from the substrate was collected using a scintillation detector in a symmetric reflection configuration at $2\theta \approx 65^\circ$. The thin film sample was vacuum held onto a motorized, high precision XYZ stage. The position of the shocked region relative to the X-ray beam was carefully calibrated. Then, by scanning the sample relative to the beam in 4 or 2 microns spacing, the distribution of the Si(004) intensity across the shocked region was recorded. Samples of three thicknesses treated at various conditions were tested.

4.2 Results and Discussions

Fig. 5(a) shows the profiles of Si (004) diffraction intensity contrast across the shocked region by a line of shocks of the 1 μ m sample. The diffraction intensity is normalized to the background diffraction intensity. All the measurements were taken at 2 microns spacing. Although some fluctuations exist in the diffraction profile, large central peaks were detected for both 244 μ J and 209 μ J samples, and the magnitude agrees with the trend in simulation: the higher the diffraction intensity, the stronger the shock load. The peaks are 1.8 and 1.4 for 244 μ J and 209 μ J, respectively, while the half-widths of the peaks are 30-40 microns. For both cases, the X-ray intensity contrast reflects the stress/strain concentration in the shocked region.

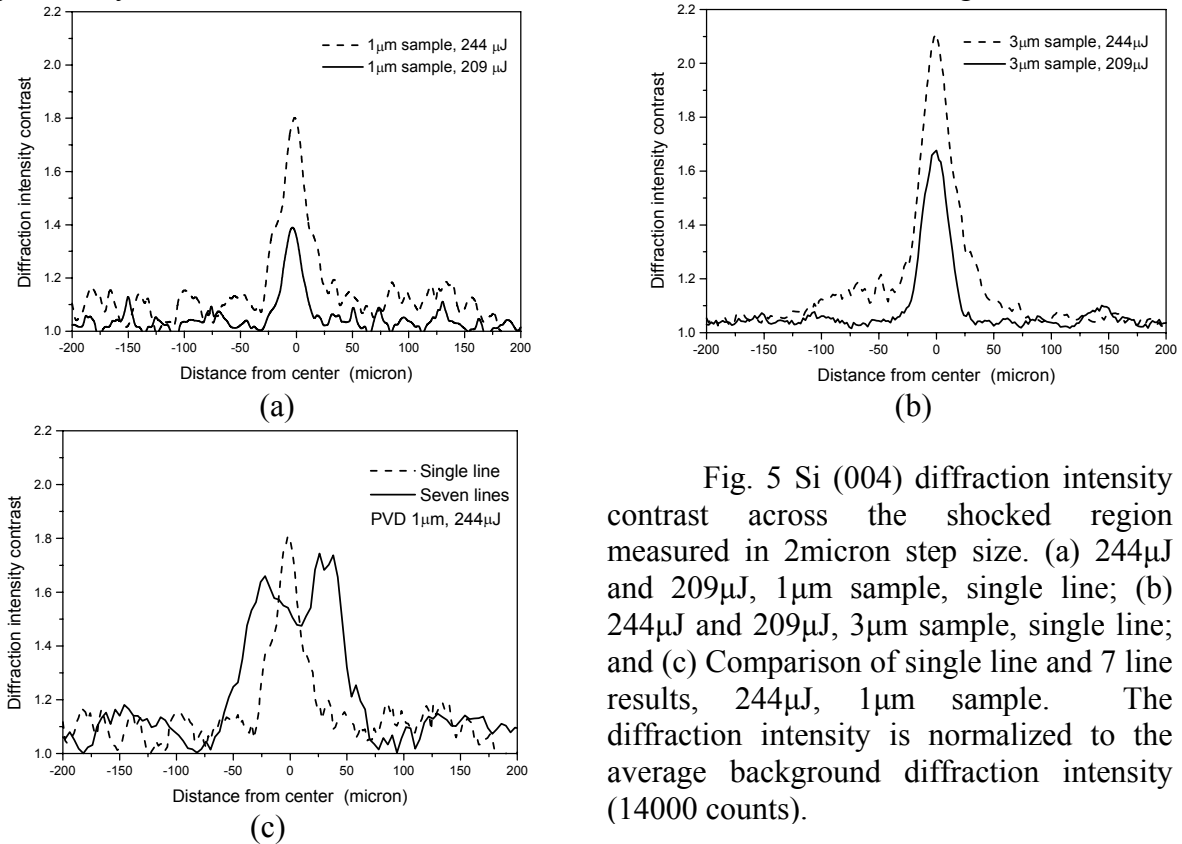


Fig. 5 Si (004) diffraction intensity contrast across the shocked region measured in 2micron step size. (a) 244 μ J and 209 μ J, 1 μ m sample, single line; (b) 244 μ J and 209 μ J, 3 μ m sample, single line; and (c) Comparison of single line and 7 line results, 244 μ J, 1 μ m sample. The diffraction intensity is normalized to the average background diffraction intensity (14000 counts).

The intensity contrast profiles for 3 μm samples processed at 244 μJ and 209 μJ are shown in Fig. 5(b). A similar trend as in the 1 μm sample is observed. However, under the same energy levels, the intensity contrasts of the 3 μm sample are larger than those of the 1 μm sample. This reveals that a stronger local strain field is induced in thicker films under the same conditions. The rising diffraction intensity profile is due to shock effects, as further verified by the comparison of the results of single line and 7 lines for the 1 μm sample at 244 μJ (Fig. 5(c)). The profile of the 7 lines case shows a much wider central rising part than the single line case, covering a region about 150 microns, which is close to the total span of shock treated region.

The location of stress/strain concentration and relative change of stress/strain in metal thin film can be inferred from the diffraction contrast of the substrate (Wang et al., 2000), but the quantitative correspondence between local stress/strain and the increase in diffraction intensity is a complex problem and is still under investigation. In experiments, it is difficult to find a suitable and measurable index to represent the degree of imperfection of the lattice. Efforts had been made to correlate strain or stress components in simulations directly with the X-ray diffraction intensity contrast. But the width of elastic strain or residual stress in the film is much greater than the width of the rising peaks in Fig. 5, while the width of plastic strain in simulation is less than the peaks in Fig. 5. Going back to the origination of the X-ray diffraction intensity contrast, the increase of diffraction intensity comes from the increased mosaic structure in the substrate induced by the stress/strain field in the thin film at the interface. An index evaluating this combined effect is strain energy density D which is defined as:

$$D = \frac{1}{2} \varepsilon_{ij} \sigma_{ij} = \frac{1}{2} (\varepsilon_{11} \sigma_{11} + \varepsilon_{22} \sigma_{22} + \varepsilon_{33} \sigma_{33} + \varepsilon_{12} \sigma_{12} + \varepsilon_{13} \sigma_{13} + \varepsilon_{23} \sigma_{23}) \quad (2)$$

where ε_{ij} is the total strain (elastic plus plastic) tensor and σ_{ij} the residual stress tensor. The unit of D is J/m^3 .

Profiles of X-ray diffraction intensity contrast of single line shock processed 1 μm and 3 μm samples are compared with the profiles of strain energy density in Fig. 6(a) and (b), respectively. The profiles from simulation and from X-ray experiment come into good agreement when the Y-axes are properly adjusted. For the single line case, both 1 μm and 3 μm samples show a single central peak. For the 7-lines case of the 1 μm sample, however, both the intensity contrast in the X-ray experiment and the strain energy density in simulation show a rising saddle peak (Fig. 6(c)). Simulation predicts a slightly wider distribution of the central rising part than X-ray experiments, but the difference is within the range of experimental error. Stress/strain is relatively uniform within the directly shocked region in the case of 7-lines, but the transition from a uniformly shocked region to a shock free region results in stress concentration. Strain energy density increases in these transitional regions, which is the cause of the saddle shape in Fig. 6(c).

The fact that peak location and peak shape show good agreement simultaneously indicates that the two quantities may be linearly related. Let XDC be the X-ray diffraction intensity contrast. From Fig. 11, an empirical relation is inferred:

$$D \approx K(XDC - 1) = \frac{\max(D)}{\max(XDC - 1)} (XDC - 1) \quad (3)$$

where K is a proportional coefficient. This linear correlation is relatively well obeyed for other conditions as well. The linear correlation between strain energy density and X-ray

microdiffraction contrast makes it possible to decide the strain field gradient directly from the measurement of X-ray diffraction intensity contrast.

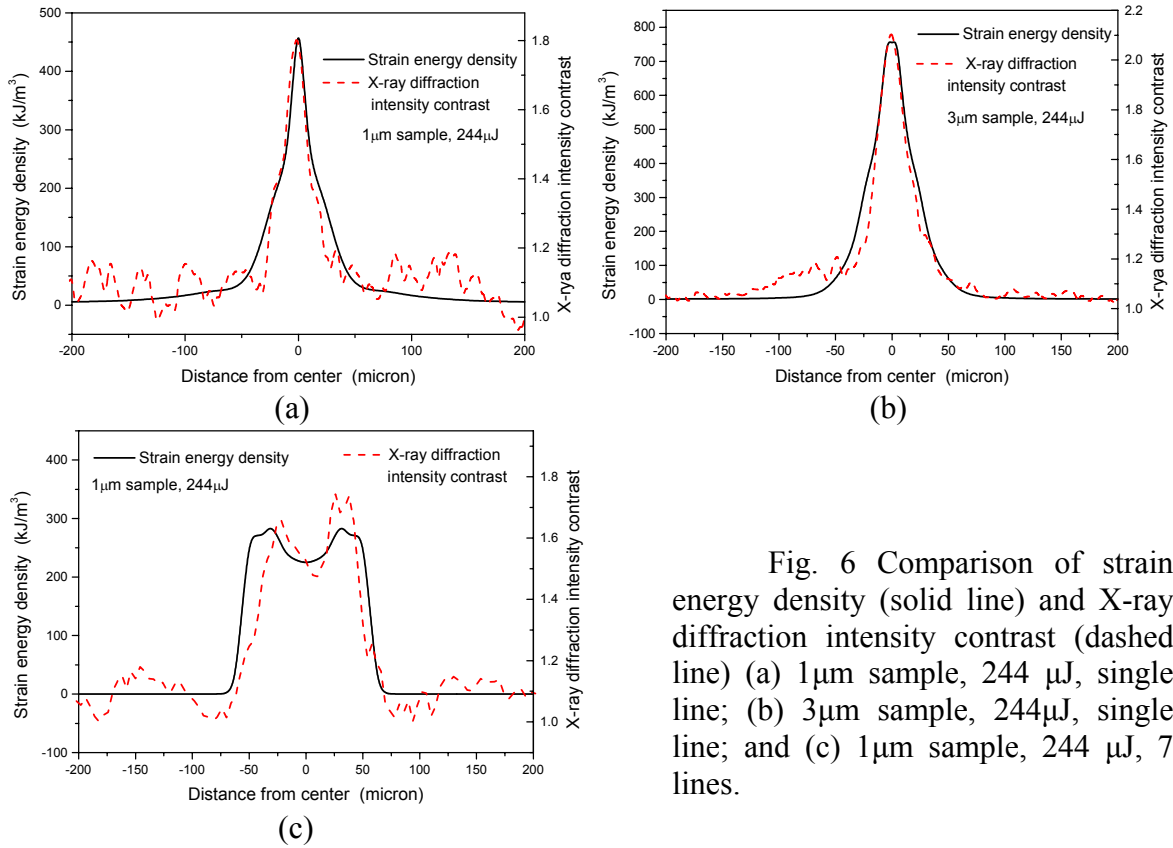


Fig. 6 Comparison of strain energy density (solid line) and X-ray diffraction intensity contrast (dashed line) (a) 1 μm sample, 244 μJ , single line; (b) 3 μm sample, 244 μJ , single line; and (c) 1 μm sample, 244 μJ , 7 lines.

5 Conclusions

Microscale laser shock processing can induce compressive in-plane stress distributions in the thin films on silicon substrate as proven by the wafer curvature measurements and 3D stress/strain simulations. The compressive residual stress distribution is beneficial for the prevention of micro-crack initiation and propagation. The stress/strain field in the thin film is coupled to the silicon substrate and the silicon substrate is elastically deformed in the shock-affected region. X-ray microdiffraction measurements based on intensity contrast method successfully detected the region of stress/strain concentration with micron-level spatial resolution. It was found that X-ray diffraction intensity contrast might be linearly related to the strain energy density at the film interface.

Acknowledgement

Valuable discussions with Prof. I. C. Noyan and Prof. D. N. Beshar are greatly appreciated. Assistance in X-ray microdiffraction experiments by Dr. S. K. Kaldor, Prof. I. C. Noyan, and Dr. J. L. Jordan-sweet are also greatly appreciated.

References

Chang, C. and Chang, P., 2000, "Innovative Micromachined Microwave Switch with Very Low Insertion Loss," *Sensors and Actuators A: Physical*, Vol. 79(1), Jan. 25, 2000, pp. 71-75.

Noyan, I. C., Jordan-sweet J. L., Liniger, E. G., Kaldor, S. K., 1998, "Characterization of Substrate / Thin-film Interfaces with X-ray Microdiffraction," *Applied Physics Letters*, Vol., 72(25), pp. 3338-3340.

Noyan, I. C., Wang, P. -C, Kaldor, Jordan-sweet, J. L., and Liniger, E. G., 2000, "Divergence Effects in Monochromatic X-ray Microdiffraction Using Tapered Capillary Optics," *Review of Science Instruments*, Vol. 71(25), pp. 1991-2000.

Segmüller, A., Angilelo, J., and La Placa, S. J., 1980, "Automatic X-ray Diffraction Measurement of the Lattice Curvature of Substrate Wafers for the Determination of Linear Strain Patterns," *J. Appl. Phys.*, Vol. 51(12), pp. 6224-6230.

Wang, P. -C., Noyan, I. C., Kaldor, S. K., Jordan-sweet, J. L., Liniger, E. G., and Hu, C. -K., 2000, "Topographic Measurement of Electromigration-induced Stress Gradients in Aluminum Conductor Lines," *Applies Physic Letters*, Vol. 76(25), pp. 3726-3728.

Walraven, J. A., Mani, S. S., Fleming, J. G., Headley, T. J., Kotula, P. G., Pimentel, A. A., Rye, M. J., Tanner, D. M., and Smith, N. F., 2000, "Failure Analysis of Tungsten Coated Polysilicon Micromachined Microengines," *MEMS Reliability for Critical Applications, Proceedings of SPIE*, Vol. 4180 (2000), pp. 49-57.

Zhang, W. and Yao, Y. L., 2002, "Micro Scale Laser Shock Processing of Metallic Components," *ASME Journal of Manufacturing Science and Engineering*, Vol. 126, No. 2, pp. 369-378.

Zhang, W. and Yao, Y. L., 2001, "Modeling and Simulation Improvement in Laser Shock Processing," *Proc. ICALEO 2001*, Section A.

Meet the Authors

Wenwu Zhang has a PhD in Mechanical Engineering from Columbia University and is currently with General Electric Global Research Center, where he works on non-traditional manufacturing R&D. Y. Lawrence Yao is a Professor of Mechanical Engineering and Director of Manufacturing Research Lab at Columbia University, where his research group works on laser shock peening, laser forming, and laser micromachining. Yao has a Ph.D. from the University of Wisconsin-Madison.

